

Study on the Passive Film of Type 316 Stainless Steel

Jong Jip Kim* and Yu Mi Young

Korea Research Institute of Standards and Science, Doryong dong 1, Yusong, TaeJon, 305-600, Korea
*E-mail: jjkim@kriss.re.kr

Received: 3 July 2013 / Accepted: 15 August 2013 / Published: 10 September 2013

The passive films of type 316 stainless steel formed in NaCl solutions were investigated by potentiodynamic polarization, electrochemical impedance measurement and Mott-Schottky analysis. The passive films are composed of p-type and n-type layers regardless of the presence of negative resistance in the films. With increasing the time and potential for film formation, thicker and more protective films are formed, with no evidence of chloride penetration. In addition, the charge carrier densities are affected by the content of dissolved oxygen, suggesting that chemical species necessary for passivation are provided by dissolved oxygen.

Keywords: Passive film, EIS, polarization, Mott-Schottky analysis

1. INTRODUCTION

Stainless steels have excellent corrosion resistance due to the presence of protective passive films. The films consist of either metal oxides or hydroxides and act as a barrier protecting the metal surface from the corrosive environment.

The passive films of stainless steels are known to be highly doped semiconductors with dopant or defect density in the range of 10^{20} to 10^{21} cm^{-3} [1-4]. The dopants in semiconducting passive films include cation vacancies, anion vacancies and cation interstitials. Semiconducting behavior is dependent upon the predominant defect present in the passive oxide layer. Oxygen vacancies and cation interstitials acting as electron donor impart n-type conductivity to the passive layer, while cation vacancies acting as electron acceptor produce a p-type layer [5]. A typical passive film of stainless steels has a double layer structure [3,6]. The inner region is composed of a p-type chromium oxide, and the outer region consists of an n-type iron oxide with hydroxide near the solution.

The composition of passive films formed by potentiostatic polarization varies with the pH of the solution used for the formation of film. In austenitic stainless steels, iron oxides are readily formed

in alkaline solutions, whereas chromium rich oxide is favorably formed in acidic solutions [7,8].

The protectiveness of the passive film is affected by the density of dopants or charge carriers. The charge carrier density is dependent upon the potential applied in polarization for film formation. In general, the density is decreased with increase in applied potential leading to the improvement in the protective ability of the passive film. However, for the passive film formed on an austenitic stainless steel in solutions containing Cl^- ions, increase in applied potential has also been reported to increase the charge carrier density caused by the penetration of Cl^- through the passive film [8]. Chloride ions were detected in the passive films [9] in contrast with the prediction of point defect model (PDM) [10,11], and the passive film growth data against the PDM was also presented in the work for another austenitic stainless steel (type 316 stainless steel) in chloride containing solutions [12].

Other factors that influence the charge carrier density are the pH, content of dissolved oxygen of solution and time of polarization for film formation. Effects of these factors in austenitic stainless steels have been reported mostly on passive films formed in neutral, alkaline and acidic solutions containing sulfide and sulfate ions [8, 9, 13-15]. In addition, effects of dissolved oxygen on charge carrier density were reported to be inconsistent. The increase of dissolved oxygen content increased the charge carrier density in type 316L stainless steel [16], whereas no obvious change was found for type 304 stainless steel in chloride containing solutions [17]. Thus, more work is needed to examine the effects of the factors affecting the semiconducting properties of austenitic stainless steels, especially, in chloride containing acidic solutions.

In the present work, the semiconducting properties of the passive film formed on type 316 stainless steel by potentiostatic polarization in neutral and acidic NaCl solutions were studied by potentiodynamic polarization, electrochemical impedance spectroscopy (EIS) and capacitance (Mott-Schottky) measurements. Type 316 stainless steel was chosen as the specimen material because it is an austenitic stainless steel with high resistance to chloride attack, which is often used in marine applications.

2. EXPERIMENTAL PROCEDURE

2.1. Specimen preparation

A commercial, type 316 stainless steel plate was used in this investigation. The chemical composition is by weight: 0.08 C, 0.44 Si, 0.42 Mn, 0.025 P, 0.001 S, 16.72 Cr, 13.23 Ni, 0.03 Mo and Fe balance. The plate was annealed for 3600 s at 1080 °C and quenched in water. Disc-type specimens 16 mm in diameter were cut from the plate and mechanically ground to have a thickness of 2 mm. The ground surfaces of specimens were polished finally using 1 μm diamond paste. Specimens were then mounted in a flat specimen holder sealed with a crevice free gasket.

2.2. Electrochemical measurement

Polarization and electrochemical impedance measurements were carried out at 22 ±2 °C in

either neutral ($\text{pH} = 6.9$) or acidic ($\text{pH} = 1.6$, acidified by HCl) 0.35 M NaCl solutions. A conventional three electrode cell was used in a 1 L flask with specimen electrode, platinum counter electrode and saturated calomel electrode. The measurement system employed was G300 (Gamry Instruments) driven by DC105 and EIS 300 softwares.

For most of tests, the solution electrolyte was deaerated before specimen immersion with a pure nitrogen gas, which continued throughout the test. Corrosion potential was measured for 1 hr prior to potentiodynamic, potentiostatic and electrochemical impedance measurements. The potentiodynamic polarization curves were obtained at a scan rate of 0.6 V/h, and potentiostatic polarization was conducted at constant potentials more positive than corrosion potential by 300 and 350 mV. The EIS data were acquired in the frequency range from 100 kHz to 10 mHz with an amplitude of 10 mV peak to peak for the a.c. signal.

2.3. Mott-Schottky measurement

Mott-Schottky (M-S) measurements were carried out immediately after obtaining passive films grown by potentiostatic polarizations. The measurements were initiated first at the final passivation potential, and then scanned as a function of decreasing 50-mV potential steps in the cathodic direction down to -1200 mV with respect to passivation potential using EIS 300 software (Gamry Instruments). An a.c. voltage signal of 10 mV amplitude at 1 kHz was applied for the measurements.

The relationship between the capacitance and applied potential used for analysis is given by M-S equations [2,18].

$$1/C^2 = 2(E_{FB} - E + kT/q)/\epsilon\epsilon_0 q N$$

where ϵ is the dielectric constant of the passive film, ϵ_0 the permittivity of free space (8.858×10^{-14} F/cm), q the electron charge (1.602×10^{-19} C), N the charge carrier density, E_{FB} the flat band potential, k the Boltzmann constant (1.38×10^{-23} J/K) and T the absolute temperature. The charge carrier density N was determined from the slope of the $1/C^2$ vs. applied potential assuming the dielectric constant of the passive film on the stainless steel as 15.6 [19].

3. RESULTS AND DISCUSSION

3.1. Potentiodynamic polarization

Fig. 1 shows the potentiodynamic polarization curves of type 316 stainless steel obtained after immersion for 3600 s in deaerated 0.35 M NaCl solution. A current plateau is seen with a well defined anodic peak in deaerated acidic solution ($\text{pH} = 1.6$), but no peak in deaerated neutral ($\text{pH} = 6.9$) solution. The rising part of the curve in the former represents active dissolution, and the falling part reveals active-passive transition. The current plateau indicates the presence of passive region in both solutions. Corrosion potential was shifted to a more noble value, and current level in both active and

passive regions was lower in neutral solution.

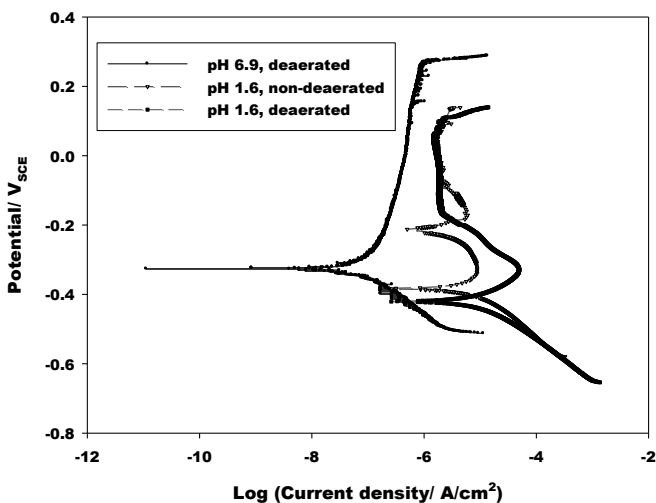


Figure 1. Potentiodynamic polarization curves after immersion for 3600 s in deaerated and non-deaerated solutions.

In non-deaerated acidic solution, a cathodic loop is observed in anodic polarization in addition to the conventional active-passive transition. This has been reported for Cr and Cr alloys in dilute sulfuric and chloride containing acidic solutions and was ascribed to hydrogen evolution reaction proceeding on the passive surface, which results in a second stable corrosion potential in the passive region [20,21]. Values of current density in the passive region were higher in non-deaerated acidic solutions compared to those in deaerated acidic solutions.

3.2. Electrochemical Impedance Spectra

Fig. 2 presents the EIS Nyquist plots obtained after immersion for 3600 s under open circuit conditions in 0.35 M NaCl solutions. The Nyquist plots are composed of capacitive arcs in all solutions, but with different diameters. The arc represents the combined effects of electric double layer capacitance C_{dl} and charge transfer resistance R_{ct} , and its diameter is related to the magnitude of charge transfer resistance at the metal-solution interface. Values of resistance and capacitance could be determined by fitting to an equivalent circuit consisting of solution resistance R_s in series with the parallel combination of the C_{dl} and R_{ct} with a constant phase element Q_{dl} replacing the C_{dl} .

As can be seen in table 1, the value of R_{ct} was much higher, but that of Q_{dl} was much lower in deaerated neural solution than those in deaerated acidic solution indicating corrosion rate under open circuit condition would be much lower in the former due to passivation. In addition, value of R_{ct} was higher in non-deaerated acidic solution, but that of Q_{dl} was lower than in deaerated acidic solution, indicating that corrosion rate under open circuit condition would be lower in non-deaerated solution.

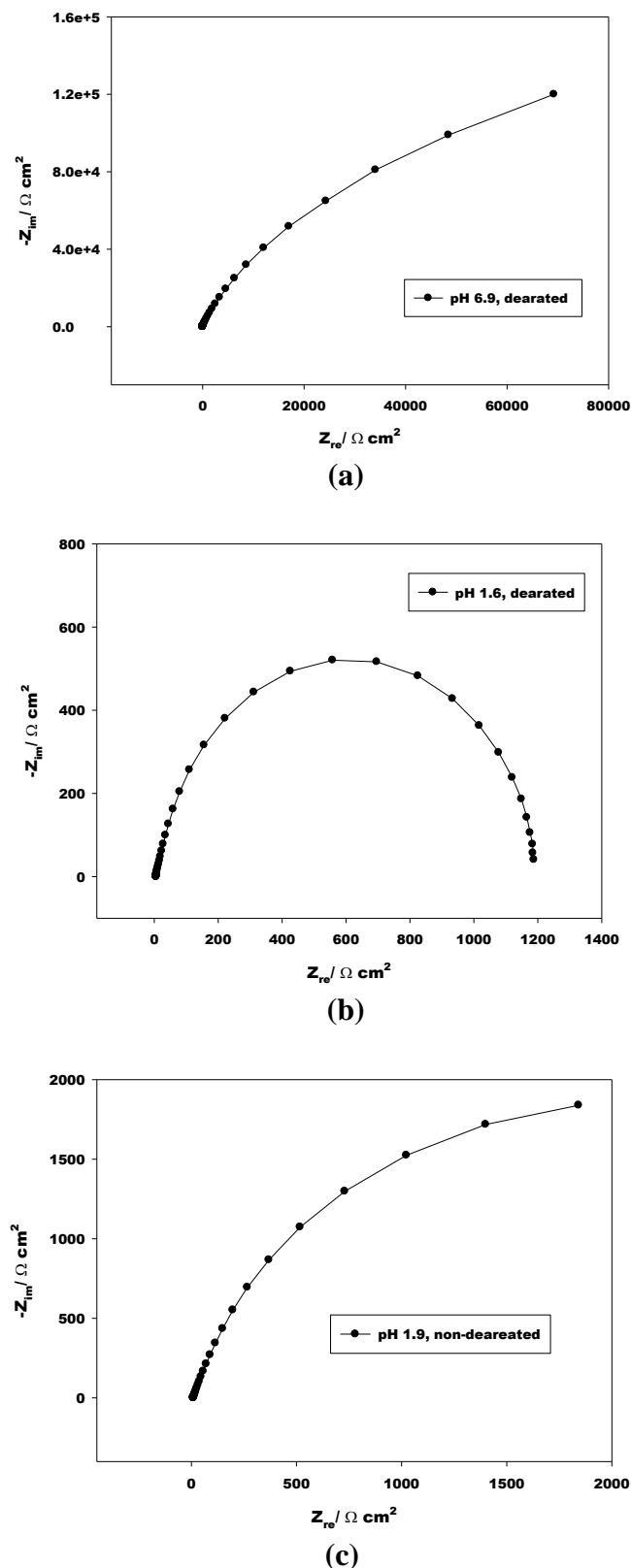
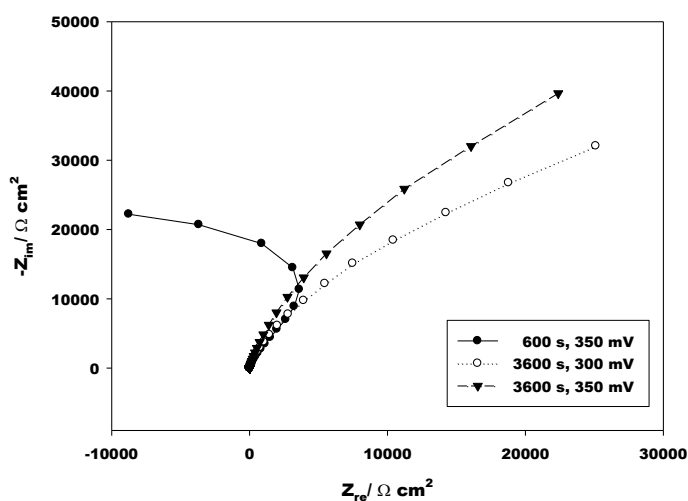


Figure 2. Nyquist plots after immersion for 3600 s under open circuit conditions in deaerated neutral (a), deaerated acidic (b) and non-deaerated acidic (c) solutions.

Table 1. Values of R_{ct} and Q_{dl} under open circuit condition.

Solution	$R_{ct} (\Omega \cdot \text{cm}^2)$	$Q_{dl} (\text{F}/\text{cm}^2)$
pH 6.9, deaerated	3.9×10^5	7.5×10^{-5}
pH 1.6, deaerated	1222	2.4×10^{-4}
pH 1.6, non-deaerated	5567	1.3×10^{-4}

Fig. 3 shows the impedance spectra taken after passivation at potentials of 300 and 350 mV more positive than corrosion potentials in deaerated acidic solutions ($\text{pH} = 1.6$). Semicircles running in opposite directions are seen in the spectra. For the specimens passivated for 600 s at a potential 350 mV more positive than corrosion potential, a circle in the high frequency region is related to the typical impedance due to charge transfer. Another circle in the low frequency region running up and left represents the so-called negative resistance, which has been reported in previous works [23-26]. Thus, negative resistance is observed at the beginning of passivation even in the passive region unlike in earlier reports in which it was observed only in the active-passive transition region. The negative resistance was attributed to the adsorption of bond water [25] in a stainless steel or the progressive passivation of the electrode surface by the formation of Ni(OH)_2 in Ni [26]. The spectrum could be best fitted by the equivalent circuit consisting of R_s in series with the parallel combination of the R_{ct} and Q_{dl} which is also in series with another parallel combination of a resistance R_{ad} and a CPE Q_{ad} of the adsorbed layer.

**Figure 3.** Nyquist plots after passivation in a deaerated acidic solution ($\text{pH}=1.6$) at potentials 300 and 350 mV more positive than corrosion potential.

After passivation for 3600 s at potentials 300 and 350 mV more positive than corrosion potential, the spectra consist of semicircles running up and right. The spectra could be best fitted by the equivalent circuit consisting of R_s in series with the parallel combination of the R_{ct} and Q_{dl} , and the

value of R_{ct} is in the order of 10^5 ohm-cm 2 as shown in Table 2, indicative of the formation of protective passive layer.

In addition, the value of charge transfer resistance increases, but that of capacitance decreases with increasing either the potential or time for passivation. This indicates that the passive film becomes more protective as either the time or potential for passivation is increased

Table 2. Values of resistance and CPE after passivation at potentials 300 and 350 mV more positive than corrosion potential.

Condition	R_{ct} ($\Omega\text{-cm}^2$)	Q_{dl} (F/cm^2)	R_{ad} ($\Omega\text{-cm}^2$)	Q_{ad} (F/cm^2)
3600 s, 300 mV	9.0×10^4	1.8×10^{-4}		
600 s, 350 mV	4.5×10^4	2.0×10^{-4}	-3.1×10^4	2.4×10^{-4}
3600 s, 350 mV	1.5×10^5	1.4×10^{-4}		

Fig. 4 compares the impedance spectra after passivation for 3600 s at a potential 350 mV more positive than corrosion potential in neutral (pH = 6.9) and acidic (pH = 1.6) solutions. The charge transfer resistance of the passive film formed in deaerated neutral solution was higher but with lower values of capacitance than those formed in deaerated acidic solution as summarized in table 3. This is attributed to the formation of thicker and more protective film after passivation in deaerated neutral solution.

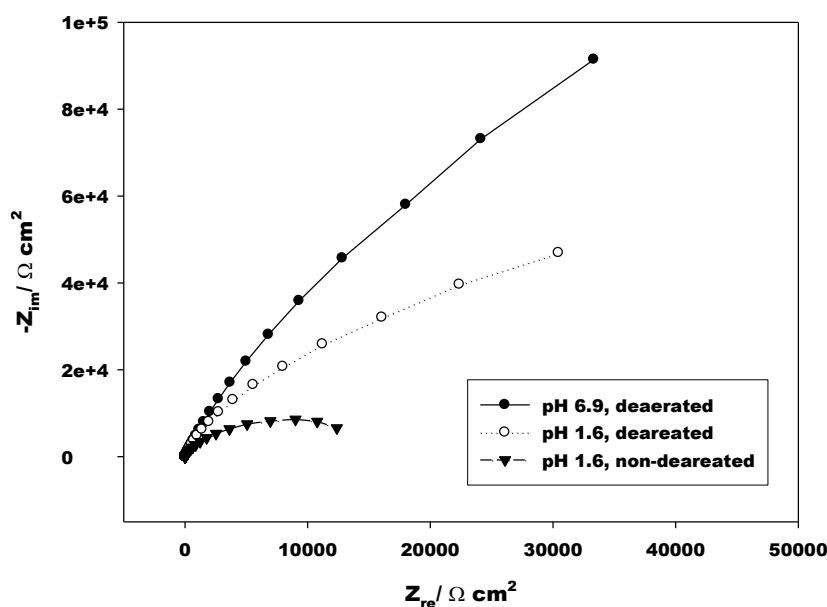


Figure 4. Nyquist plots after passivation for 3600 s at a potential 350 mV more positive than corrosion potential in neutral (pH=6.9) and acidic (pH=1.6) solutions.

In addition, the charge transfer resistance of the passive film formed in non-deaerated acidic

solution was lower but with higher value of capacitance than those formed in deaerated acidic solution. This indicates that passive films formed in acidic solution with higher content of dissolved oxygen is thinner and less protective than those formed in acidic solution with lower content of dissolved oxygen.

Table 3. Values of resistance and CPE after passivation in three solutions for 3600 s at a potential 350 mV more positive than corrosion potential.

Solution	$R_{ct} (\Omega \cdot \text{cm}^2)$	$Q_{dl} (\text{F}/\text{cm}^2)$
pH 6.9, deaerated	5.7×10^5	5.2×10^{-5}
pH 1.6, deaerated	9.0×10^4	1.4×10^{-4}
pH 1.6, non-deaerated	2.4×10^4	1.8×10^{-4}

3.3. Mott-Shottky analysis

Fig. 5 shows the semiconducting behavior of the passive films formed in deaerated acidic solutions for 3600 s at potentials of 0.30 V and 0.35 V more positive than corrosion potential. The plots exhibit two linear regions with a negative and a positive slope separated by narrow potential plateau region characteristic of flat band potential. The region of the straight line with a negative slope indicates the presence of p-type semiconducting behavior, and that of the straight line with a positive slope indicates the presence of n-type semiconducting behavior in the passive film. The shape of plots is similar to that reported for passive films formed on stainless steels [2,3,19]. The p-type semiconducting behavior has been attributed to chromium oxides in the inner layer, and n-type semiconducting behavior has been explained as due to iron oxides in the outer layer [3,19].

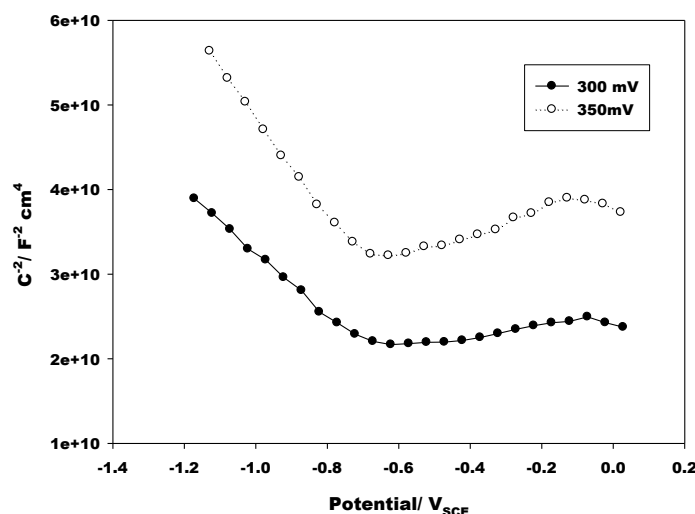


Figure 5. M-S plots of the passive films formed after passivation in a deaerated, acidic solution for 3600 s at potentials of 0.30 V and 0.35 V more positive than corrosion potential.

The charge carrier densities of acceptor N_a and donor N_d were calculated from the slope of the straight lines of M-S plots. The values of N_a and N_d are in the order of 10^{20} cm^{-3} for the passive films formed at both potentials, which are comparable to the reported values for the passive films of stainless steels [1-4]. Charge carrier density is related to the non-stoichiometry, defect in space charge region or disordered character of the passive film [3,19], and donors or acceptors in semiconducting passive layers are defect themselves. Dominant acceptor species in p-type passive film are cation vacancy, and dominant and detectable donor species in n-type semiconductor are oxygen vacancy and cation interstitial [5,27]. Presence of such dopants is known to prevent the migration of cations from substrate metals and the penetration of anions from the electrolyte, resulting in the improvement of corrosion resistance [28,29].

As can be seen in Table 4, both N_a and N_d are decreased by increasing the passivation potential from 300 mV to 350 mV with respect to the free corrosion potential. Decrease in values of N_a and N_d is attributed to the formation of thicker or more protective passive films after passivation at 350 mV than at 300 mV with respect to the free corrosion potential. This is consistent with the EIS results (Fig. 3) and is also manifested by the values of capacitance for all range of potentials which are lower after passivation at 350 mV with respect to the free corrosion potential.

Table 4. Acceptor and donor densities after passivation under various conditions.

Passivation condition	$N_a (\text{cm}^{-3})$	$N_d (\text{cm}^{-3})$
300 mV, 3600 s, deaerated, pH 1.6	2.5×10^{20}	9.7×10^{20}
350 mV, 600 s, deaerated, pH 1.6	1.9×10^{20}	1.2×10^{21}
350 mV, 3600 s, deaerated, pH 1.6	1.6×10^{20}	2.6×10^{20}
350 mV, 10800 s, deaerated, pH 1.6	9.5×10^{19}	2.4×10^{20}
350 mV, 3600 s, deaerated, pH 6.9	6.1×10^{19}	2.1×10^{20}
350 mV, 3600 s, non-deaerated, pH 1.6	1.5×10^{20}	1.1×10^{21}

Thus, the effect of chloride ion penetration is not seen in contrast with an earlier work [8]. The charge carrier density of the passive films of a high nitrogen austenitic stainless steel in acidic NaCl solutions has been reported to increase with the increase in potential for passivation. This was attributed to the increased penetration force for the Cl^- through passive film. The chloride ions were shown to take part in the formation of the passive film and were detected in the passive films of nitrogen containing stainless steels. Detection of chloride ions in the passive film was used as an evidence to contradict the point defect model since Cl^- is postulated to act only at the passive film/solution interface and neither penetrates nor incorporates into the passive film in the model [10,11].

Fig. 6 presents the effects of time for passivation on the semiconducting behavior of the passive films formed in deaerated acidic solution at a potential of 0.35 V more positive than corrosion potential. The shape of plots is similar to that in Fig. 5. Both the p-type and n-type semiconducting behavior are seen in all passive films, regardless of whether the negative resistance is observed. Note that negative resistance was observed only for the passive film passivated for 600 s. In addition, no significant

difference in E_{FB} is found between the passive films with negative and positive resistance, implying that the composition of the films is similar. This indicates that the films formed by passivation for 600 s is thinner and less protective, but with no significant difference in composition.

The charge carrier density decreases with time for passivation as was shown in table 4, indicating that the passive film continues to grow and becomes more protective with time. Also noted is the decrease in capacitance with time for all potential range (Fig. 6), which also confirms that the film becomes more compact so that the protective characteristic is improved with time for passivation.

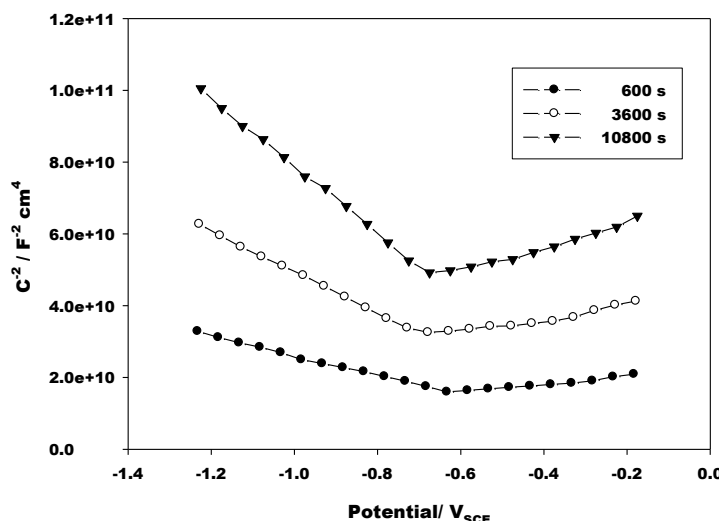


Figure 6. Effects of time for passivation on the semiconducting behavior of the passive films formed in deaerated, acidic solution at a potential of 0.35 V more positive than corrosion potential

Fig. 7 shows the effects of pH on the semiconducting behavior of the passive films formed in deaerated acidic solutions at a potential of 350 mV more positive than corrosion potential.

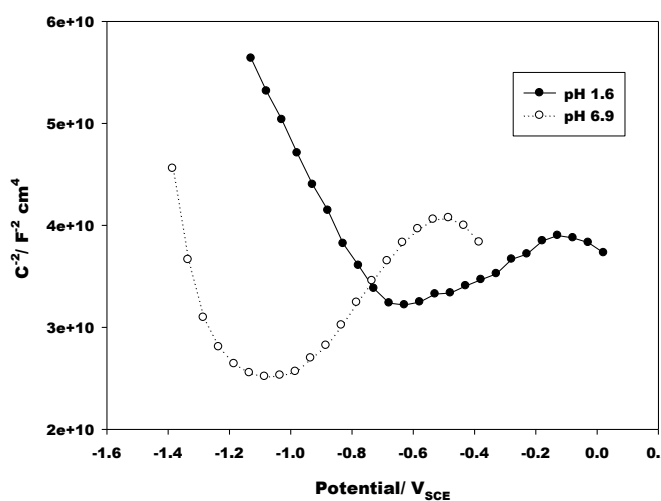


Figure 7. Effects of pH on the semiconducting behavior of the passive films formed in deaerated acidic solutions after passivation for 3600 s at a potential of 350 mV more positive than corrosion potential.

The charge carrier densities of n-type and p-type are lower for the passive film formed in deaerated neutral solutions (table 4), compared to those in deaerated acidic solutions. This is consistent with the results of EIS (Fig. 4), in which the charge transfer resistance is higher, but the capacitance is lower in deaerated neutral solutions compared to those in deaerated acidic solutions. The decrease in charge carrier densities with pH is attributed to the thicker passive film formed in the former. According to the PDM, a linear dependence of the oxide thickness on pH is predicted [30]. As the pH is increased, less oxygen vacancies are created and the charge carrier density is decreased.

Also noted is the shift of the flat band potential E_{FB} which suggests the formation of passive films with different compositions in these solutions though the compositions were not identified in this work. The difference in E_{FB} values was explained as due to the difference in the affinity of absorption or adsorption of anions in the passive film [9]. The composition of passive film has also been reported to vary with the pH of the solution for film formation [4,31]. In acid solutions, chromium rich oxide film is more likely to be formed due to slower dissolution of chromium oxide than iron oxide [13, 31].

Fig. 8 presents the effects of dissolved oxygen on the semiconducting behavior of the passive films formed for 3600 s at a potential of 350 mV more positive than corrosion potential. Charge carrier density of n-type is higher for the passive film formed in non-deaerated solution compared to that formed in deaerated solution (table 4), but no remarkable difference is observed in charge carrier density of p-type. This indicates that the change in content of dissolved oxygen affects the density of oxygen vacancies and cation interstitials, but not that of cation vacancies significantly in the passivation condition employed in the present work.

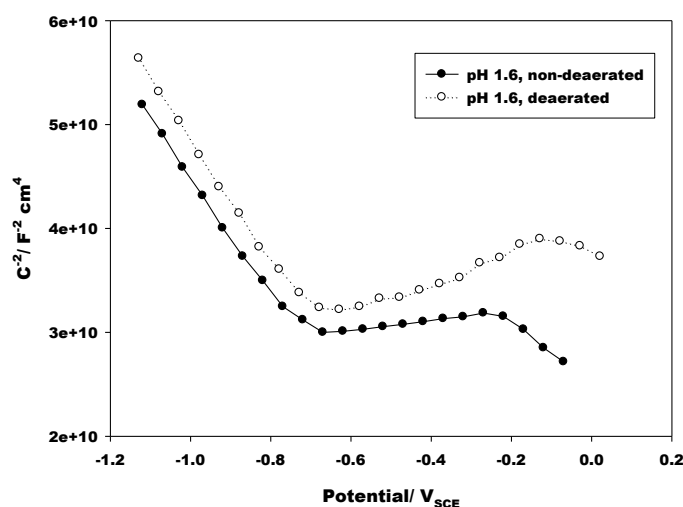


Figure 8. Effects of dissolved oxygen on the semiconducting behavior of the passive films formed for 3600 s at a potential of 350 mV more positive than corrosion potential.

For the passive films formed for 3600 s, only the outer n-type layer may be affected by the increase in the content of dissolved oxygen. Higher charge carrier density in the passive layer formed in solutions with greater dissolved oxygen content is consistent with the EIS results (Fig. 4) in which

lower charge transfer resistance but higher capacitance value were obtained for the specimens passivated in non-deaerated solution. This was attributed to the formation of less compact and protective passive film in non-deaerated solution. The effect of dissolved oxygen on the defect density found in this work is in agreement with a previous work [16], but in contrast with that on austenitic stainless steels in H_2SO_4 [17]. In the former, donor density was reported to increase with dissolved oxygen for the passive film in which only n-type behavior was observed. In the latter, the passive films formed in aerated and deaerated solutions were shown to have similar charge carrier density [17]. This was explained as due to the fact that a dissolved passivating oxidizer such as dissolved oxygen apparently provides only the necessary potential for passivation but no chemical species necessary for passivation [17].

4. CONCLUSIONS

The passive films grown on AISI 316 stainless steel in NaCl solutions were investigated by potentiodynamic polarization, electrochemical impedance measurements and Mott-Schottky analysis. The passive films are composed of p-type inner layer and n-type outer layer in both neutral and acidic solutions, regardless of whether the negative resistance is observed in the films. The defect or charge carrier densities are lowered by increasing the passivation potential with no evidence of chloride penetration into the passive film in agreement with the prediction of point defect model, and the passive film is shown to continue to grow and become more protective with time. The densities were lower for the films formed in neutral solutions compared to those in acidic solutions, which is attributed to thickening of the passive film. The densities are also affected by the content of dissolved oxygen being higher for the passive film formed in non-deaerated solutions than in deaerated acidic solutions suggesting that chemical species necessary for passivation are apparently provided by dissolved oxygen.

References

1. U. Stimming and J.W. Schultze, *Electrochim. Acta*, 24 (1979) 859.
2. M.H. Dean and U. Stimming, *Corros. Sci.* 29 (1989) 199.
3. N.E. Hakiki, M.F. Montemor, M.G.S. Ferreira and M.D. Cunha Belo, *Corros. Sci.* 42 (2000) 687.
4. M.J. Carmezim, A.M. Simoes, M.O. Figueiredo and M.D. Cunha Belo, *Corros. Sci.* 44 (2002) 451.
5. D.D. Macdonald, *J. Electrochem. Soc.* 139 (1992) 3434.
6. M.F. Montemor, M.G.S. Ferreira, N.E. Hakiki and M. Da Cunha Belo, *Corros. Sci.* 42 (2000) 1635.
7. M.V. Cardoso, S.T. Amaral and E.M.A. Martini, *Corros. Sci.* 50 (2008) 2429.
8. Y.X. Qiao, Y.G. Zheng and W. Ke, P.C. Okafor, *Corros. Sci.* 51 (2009) 979.
9. S. Ningshen, U.K. Mudali, V.K. Mittal and H.S. Khatak, *Corros. Sci.* 49 (2007) 481.
10. D.D. Macdonald, *Pure Appl. Chem.* 71 (1999) 951
11. S.J. Ahn, H.S. Kwon and D.D. Macdonald, *J. Electroanal. Chem.* 579 (2005) 3111.
12. M.G.S. Ferreira and J.L. Dawson, *J. Electrochem. Soc.*, 132 (1985) 760
13. H.H. Ge, G.D. Zhou and W.Q. Wu, *Appl. Surf. Sci.* 211 (2003) 321.
14. A. Fattah-alhosseini, M.A. Golozar, A. Saatchi and K. Raeissi, *Corros. Sci.* 52 (2010) 205

15. E. Emeka, C. Oguziea, Li. Jibiao, Y.Q.Liu, D. Chen, L. Ying Li K. Yang and F. Wang, *Corros. Sci.* 51 (2009) 979.
16. Z. Feng, X. Cheng, C. Dong, L. Xu and X. Li, *J. of Nucl. Mat.* 407 (2010) 171
17. K.S. Raja and D.A. Jones, *Corros. Sci.* 48 (2006) 1623.
18. B.G. Craig (Ed.), *Fundamental Aspects of Corrosion Films in Corrosion Science*, Plenum Press, New York, 1991
19. A.M.P. Simoes, M.G.S. Ferreira, B. Rondot and M. da Cunha Belo, *J. Electrochem. Soc.* 137 (1990) 82.
20. B.E. Wilde and F.G. Hodge, *Electrochim. Acta* 14 (1969) 619.
21. L. Bjornkvist and I. Olefjord, *Corros. Sci.* 32 (1991) 231.
22. M. Bojinov, I. Betova, G. Fabricius, T. Laitinen and R. Raicheff, *J. Electroanal. Chem.* 475 (1999) 58
23. J. Mac'ak, P. Sajdl, P. Ku'cera, R. Novotn'y and J. Vo'sta, *Electrochim. Acta* 51 (2006) 3566
24. J. Gregori, J.J.G. Jareno, M. Keddame and F. Vicente, *Electrochim. Acta* 52 (2007) 7903
25. M. Slemnik, V. Dolec'ek and M. Gabers'c'ek, *Acta Chim. Slovenica*, 49 (2002) 613.
26. J. Gregori, J.J. Garc'ia-Jaren'o, D. Gim'enez-Romero and F. Vicente, *J. Sol. St. Electrochem.* 10 (2006) 920.
27. G.T. Burstein and C. Liu, *Corros. Sci.* 49 (2007) 4296.
28. E.A. Cho, H.S. Kwon and D.D. Macdonald, *Electrochim. Acta* 47 (2002) 1661.
29. N.B. Hakiki, S. Boudin, B. Rondot and M. Da Cunha Belo, *Corros. Sci.* 37 (1995) 1809.
30. D.D. Macdonald, *J. Electrochem. Soc.* 153 (2006) B213.
31. S. Haupt and H. H. Strehblow, *Corros. Sci.* 37 (1995) 43.